Research Article

EASL EUROPEAN ASSOCIATION FOR THE STUDY OF THE LIVER | JOURNAL OF HEPATOLOGY

mPGES-2 deletion remarkably enhances liver injury in streptozotocin-treated mice via induction of GLUT2

Ying Sun[1,2,†], Zhanjun Jia[1,†], Guangrui Yang[1], Yutaka Kakizoe[1], Mi Liu[1,3], Kevin T. Yang[1,3], Ying Liu[1], Baoxue Yang[2], Tianxin Yang[1,3,*]

[1]*Department of Internal Medicine, University of Utah and Veterans Affairs Medical Center, Salt Lake City, UT, United States;* [2]*Department of Pharmacology, School of Basic Medical Sciences, Peking University, Beijing, China;* [3]*Institute of Hypertension, Sun Yat-sen University School of Medicine, Guangzhou, China*

Background & Aims: Microsomal prostaglandin E synthase-2 (mPGES-2) deletion does not influence *in vivo* PGE_2 production and the function of this enzyme remains elusive. The present study was undertaken to investigate the role of mPGES-2 in streptozotocin (STZ)-induced type-1 diabetes and organ injuries.
Methods: mPGES-2 wild type (WT) and knockout (KO) mice were treated by a single intraperitoneal injection of STZ at the dose of 120 mg/kg to induce type-1 diabetes. Subsequently, glycemic status and organ injuries were evaluated.
Results: Following 4 days of STZ administration, mPGES-2 KO mice exhibited severe lethality in contrast to the normal phenotype observed in WT control mice. In a separate experiment, the analysis was performed at day 3 of the STZ treatment in order to avoid lethality. Blood glucose levels were similar between STZ-treated KO and WT mice. However, the livers of KO mice were yellowish with severe global hepatic steatosis, in parallel with markedly elevated liver enzymes and remarkable stomach expansion. However, the morphology of the other organs was largely normal. The STZ-treated KO mice displayed extensive hepatocyte apoptosis compared with WT mice in parallel with markedly enhanced inflammation and oxidative stress. More interestingly, a liver-specific 50% upregulation of GLUT2 was found in the KO mice accompanied with a markedly enhanced STZ accumulation and this induction of GLUT2 was likely to be associated with the insulin/SREBP-1c pathway. Primary cultured hepatocytes of KO mice exhibited an increased sensitivity to STZ-induced injury and higher cellular STZ content, which was markedly blunted by the selective GLUT2 inhibitor phloretin.
Conclusions: mPGES-2 deletion enhanced STZ-induced liver toxicity possibly via GLUT2-mediated STZ uptake, independently of diabetes mellitus.

Introduction

Microsomal prostaglandin E synthase 2 (mPGES-2) was initially isolated from the microsomal fraction of bovine heart [1], and the cDNAs of the human and monkey homologues were subsequently cloned [2]. This enzyme is synthesized as a Golgi membrane-associate protein, and the formation of the mature cytosolic enzyme needs proteolytic removal of the N-terminal hydrophobic domain [2,3]. mPGES-2 is constitutively expressed and most abundant in brain, heart, kidney, and small intestine [4]. Although mPGES-2 was originally found to be glutathione (GSH)-independent [2], a recent study more convincingly demonstrated the GSH-dependent property of mPGES-2 [5]. *In vivo* mPGES-2 forms a complex with GSH and haem and only haem-free mPGES-2 exhibited PGE_2 synthetic activity under *in vitro* conditions [5]. In agreement with this study, the *in vivo* evidence from mPGES-2 KO mice did not show that this protein is responsible for the PGE_2 production under basal or pathophysiological conditions [6]. Therefore, the functional role of mPGES-2 remains elusive.

The gene map of mPGES-2 is close to chromosome region 9q34.13, which is closely associated with obesity or body weight [7]. More interestingly, several recent reports strongly indicated the association of mPGES-2 arg298His polymorphism with type-2 diabetes or metabolic syndrome [8–11], which highly suggests a potential role of mPGES-2 in the regulation of energy metabolism, especially glucose metabolism.

Keywords: mPGES-2; Glucose transporter 2; Streptozotocin; Diabetes; Prostaglandin E_2.
Received 14 October 2013; received in revised form 27 June 2014; accepted 8 July 2014; available online 27 July 2014
* Corresponding author. Address: University of Utah and Veterans Affairs Medical Center, Division of Nephrology and Hypertension, 30N 1900E, RM 4C224, Salt Lake City, UT 84132, United States. Tel.: +1 801 585 5570; fax: +1 801 584 5658.
E-mail address: Tianxin.Yang@hsc.utah.edu (T. Yang).
† These authors contributed equally to this work.
Abbreviations: mPGES-2, microsomal prostaglandin E synthase 2; STZ, streptozotocin; WT, wild type; KO, knockout; GLUT2, glucose transporter 2; GSH, glutathione; COX, cyclooxygenase; HO-1, haem oxygenase 1; 15-PGDH, 15-hydroxyprostaglandin dehydrogenase; SREBP-1c, sterol regulatory element-binding protein 1c; Hct, haematocrit; PAS, Periodic acid–Schiff; EM, electron microscopy; PPAR, peroxisome proliferator-activated receptors; FAS, fatty acid synthase; HTGL, hepatic triglyceride lipase; TG, triglyceride; DGAT, diglyceride acyltransferase; TBARS, thiobarbituric acid reactive substances; ROS, reactive oxygen species; NADPH, nicotinamide adenine dinucleotide phosphate; AST, aspartate aminotransferase; ALT, alanine aminotransferase; BUN, blood urea nitrogen; AKT, protein kinase B; IR, insulin receptor.

STZ, a nitrosourea analogue, is not only a widely used reagent to reproduce the animal model of type-1 diabetes by destroying pancreatic β-cells, but is also a FDA-approved drug for the treatment of metastatic cancer of pancreatic islet cells. STZ is similar to glucose transported into cells via the glucose transporter 2 (GLUT2) rather than via other GLUTs and is particularly toxic to pancreatic β-cells due to the high expression of GLUT2, which is a well-documented fact in STZ-induced pancreatic β-cell damage in mouse and rat [12–16]. STZ induces DNA fragmentation via DNA alkylation and subsequent activation of poly ADP ribose polymerase (PARP-1) leading to the depletion of NAD (+) and ATP [17–19], which finally results in cell necrosis. Moreover, pancreatic β-cells are not the only target of STZ cytotoxicity, as DNA damage by STZ has also been found in liver and kidney cells [20].

To define the role of mPGES-2 in diabetes, we treated mPGES-2 KO mice with streptozotocin (STZ) to induce type-1 diabetes. To our surprise, mPGES-2 KO mice exhibited severe lethality and liver toxicity few days after STZ treatment, despite similar glucose levels. In the present study, we extensively characterized the hepatic phenotype of mPGES-2 KO mice and also provide the underlying mechanism, involving the change of STZ-transport by GLUT2 in the liver.

Materials and methods

Animals

mPGES-2 mutant mice were generated in our lab. This mouse colony was propagated at the University of Utah and maintained on a mixed C57/BL6x129/Sv background under a 12:12-h light-dark cycle (lights on at 6:00 a.m. and lights off at 6:00 p.m.). In all studies, 3- to 4-month-old male mice were used. All procedures were conducted according to the principles and guidance of the University of Utah Institutional Animal Care and Use Committee.

Specific methods

The methods for the generation of the STZ diabetic model, the CCl_4 liver injury model, primary hepatocyte culture, cell viability, STZ measurement, biochemical assays, DNA fragmentation, quantitative RT-PCR (qRT-PCR), Western blotting, immunohistochemistry, and statistical analysis are shown in the Supplementary data section. Primers for qRT-PCR are listed in Table 1.

Table 1. Sequences of primers for real-time PCR.

Gene	Primer sequence	Accession number
GAPDH	5'-gtcttcactaccatggagaagg-3' 5'-tcatggatgaccttggccag-3	M32599
mPGES-1	5'-agcacactgctggtcatcaa-3' 5'-ctccacatctgggtcactcc-3'	BC024960
mPGES-2	5'-gctggggctgtaccacac-3' 5'-gattcacctccaccacctga-3'	NM_133783
COX-2	5'-aggactctgctcacgaagga-3' 5'-tgacatggattggaacagca-3'	NM_011198
COX-1	5'-cattgcacatccatccactc-3' 5'-ccaaagcggacacagacac-3'	BC023322
TNF-α	5'-tccccaaagggatgagaag-3' 5'-cacttggtggtttgctacga-3'	NM_013693
MCP-1	5'-gctctctcttcctccaccac-3' 5'-acagcttctttgggacacct-3'	NM_011333
HO-1	5'-ggtgatggcttccttgtacc-3' 5'-agtgaggcccataccagaag-3'	NM_010442
p47phox	5'-gtcgtggagaagagcgagag-3' 5'-cgctttgatggttacatacgg-3'	NM_010876
p67phox	5'-ggccaagtgaaaaactactg-3' 5'-gcctcataactgaagattgc-3'	NM_010877
BAK	5′-cgctacgacacagagttcca-3′ 5′-tccatctggcgatgtaatga-3′	NM_007523
BAX	5′-tgcagaggatgattgctgac-3′ 5′-gatcagctcgggcactttag-3′	NM_007527
Caspase-3	5′-atgggagcaagtcagtgga-3′ 5′-ggcttagaatcacacacacaaag-3′	NM_009810
Glut1	5'-tcaacacggccttcactg-3' 5'-cacgatgctcagataggacatc-3'	NM_011400
Glut2	5'-tgtgctgctggataaattcgcctg-3' 5'-aaccatgaaccaagggattggacc-3'	NM_031197
Glut4	5'-gtaacttcattgtcggcatgg-3' 5'-agctgagatctggtcaaacg-3'	AB008453
DGAT1	5'-ttccgcctctgggcatt-3' 5'-agaatcggcccacaatcca-3'	NM_010046
DGAT2	5'-agtggcaatgctatcatcatcgt-3' 5'-tcttctggacccatcggccccagga-3'	NM_026384
HTGL	5'-ctgagcaccaagaagcactc-3' 5'-tggaagagcaggaatctgg-3'	X58426
FAS	5'-gctcctcgcttgtcgtct-3' 5'-gccttccatctcctgtcatc-3'	NM_007988
PPARα	5'-cgggtcatactcgcgggaaag-3' 5'-tggcagcagtggaagaatcg-3'	NM_011144

Results

The lethal phenotype of mPGES-2 KO mice following STZ treatment

To investigate the role mPGES-2 in type-1 diabetes, a single i.p. injection of STZ at 120 mg/kg was administered to WT and KO mice. Unexpectedly, after four days of STZ application, six of nine mPGES-2 KO mice died, and the remaining three were close to death. In contrast, WT mice did not show any noticeable abnormality after STZ treatment (Supplementary Fig. 1A). The six dead and three close-to death KO mice consistently exhibited a yellowish liver and an enlarged stomach, contrasting the nearly normal appearance of these organs in WT mice. The STZ-treated KO mice animals also showed lower body temperature (WT/STZ 34.2 ± 0.54 °C *vs.* KO/STZ 27.8 ± 1.61 °C, p <0.05), higher haematocrit (Hct) (WT/STZ 52.03 ± 0.84 *vs.* KO/STZ 64.13 ± 2.6, p <0.05) and lower blood glucose level (WT/STZ 436.75 ± 46.7 mg/dl *vs.* KO/STZ 272 ± 18.02 mg/dl, p <0.01), as compared with control animals or STZ-treated WT mice (Supplementary Fig. 1B–D). Liver HE staining showed mild hepatocyte oedema in WT mice but a severe global steatosis of hepatocytes in KO mice (Supplementary Fig. 1F).

To avoid lethality, a separate experimental analysis was performed at day 3 of the STZ treatment. At day 3, all STZ-treated KO mice were still alive showing a yellowish liver and enlarged stomach (Fig. 1A), as well as increased Hct (WT/STZ 51 ± 0.4% *vs.* KO/STZ 56.9 ± 1.8%, p <0.05) and slightly reduced body temperature (WT STZ/35.7 ± 0.26 °C *vs.* KO/STZ 31.86 ± 1.35 °C, p <0.05) compared to the control animals or STZ-treated WT mice, with the exception that the blood glucose increment was similar in STZ-treated WT and KO mice (WT/STZ 291.75 ± 49.53 mg/dl *vs.* KO/STZ 278.0 ± 40.77 mg/dl, p >0.05) (Supplementary Fig. 1B–D). Interestingly, mPGES-2 KO mice exhibited a significant elevation of plasma insulin levels in parallel with a

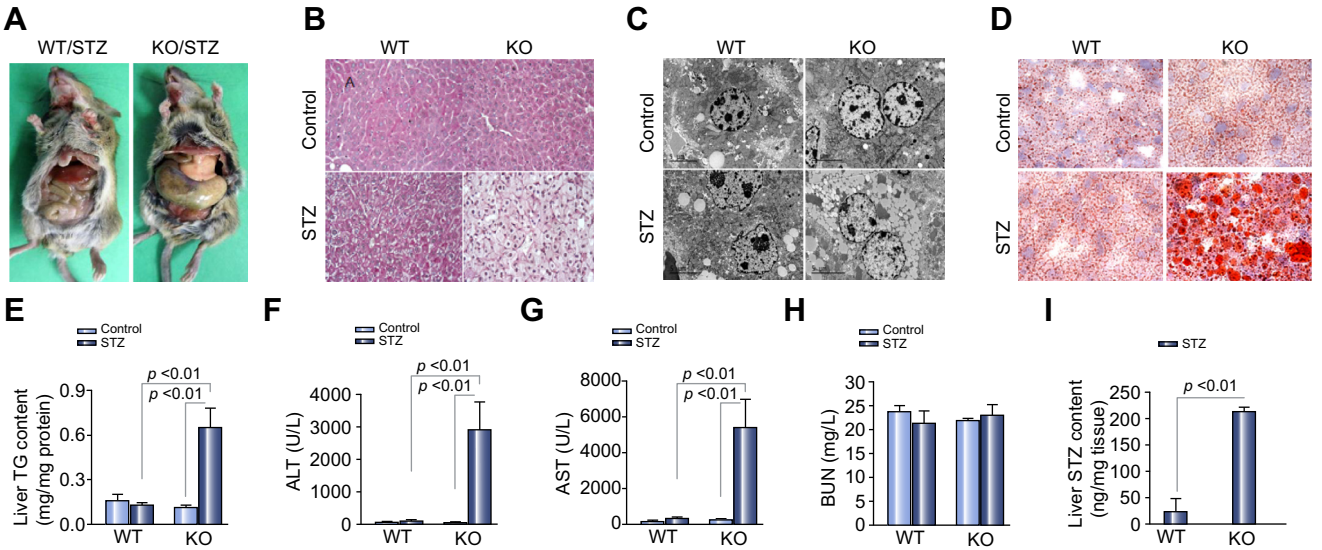

Fig. 1. mPGES-2 deletion robustly worsened liver injury and enhanced liver STZ accumulation following 3 days of STZ treatment. (A) STZ treatment led to yellowish liver and stomach enlargement in mPGES-2 KO mice. (B) PAS staining of the liver. (C) Liver electron microscopy (EM). (D) Liver Oil Red O staining. (E) Liver triglyceride (TG) content. (F) Plasma ALT concentration. (G) Plasma AST concentration. (H) Blood urea (BUN). (I) Liver STZ content. n = 5–6 per group. Data are means ± SE. (This figure appears in colour on the web.)

moderate reduction of the plasma glucose concentration under normal conditions (Supplementary Fig. 1D and E). After 3 days of STZ treatment, plasma insulin level dropped to identical levels between genotypes accompanied with similar hyperglycemia (Supplementary Fig. 1D and E). These results strongly suggest a role of mPGES-2 in pancreatic islet β-cells in controlling the insulin production and/or secretion. PAS staining, EM result, Oil Red O staining and biochemical assay of liver TG content indicated the severe global hepatic steatosis (Fig. 1B–E) and extremely thin stomach wall (Supplementary Fig. 2C) in KO mice. However, the morphology of other organs including kidney, pancreas and heart were largely normal (Supplementary Fig. 2A, B, and D). In parallel with the morphological change of the liver, liver enzymes, including plasma ALT (WT/STZ 72.7 ± 18.1 u/L *vs.* KO/STZ 2910 ± 862.1 u/L, $p < 0.01$) and AST (WT/STZ 250 ± 54.5 u/L *vs.* KO/STZ 5430 ± 1539.5 u/L, $p < 0.01$) were markedly elevated in the KO mice, but not in WT mice (Fig. 1F and G). The kidney function was evaluated by blood urea nitrogen (BUN). Neither STZ nor mPGES-2 KO affected the BUN levels (Fig. 1H).

To further clarify if STZ accumulation in the liver contributed to enhanced liver injury in KO mice, we measured liver STZ concentration on day 3 of STZ treatment. Strikingly, the STZ content in the liver of mPGES-2 KO mice was ten times higher than in WT control (Fig. 1I).

Alterations of PGE_2 and PGE_2 synthesis-related enzymes in the liver

STZ increased the liver PGE_2 content in both genotypes with a greater elevation in KO mice (WT/control 470.23 ± 89.2 *vs.* WT/STZ 1751.9 ± 388.8 pg/mg protein, $p < 0.05$; KO/control 797.6 ± 107.7 *vs.* KO/STZ 4247.6 ± 1124.5 pg/mg protein, $p < 0.05$) (Fig. 2A). The basal liver PGE_2 content tended to be higher in mPGES-2 KO mice as compared with WT controls (Fig. 2A). By qRT-PCR, none of the components of the PGE_2 synthesis pathway including *COX-1*, *COX-2*, *mPGES-1*, *mPGES-2*, *cPGES* (data not shown) or *15-PGDH* (data not shown) were significantly elevated in WT mice after STZ except for a trend in the induction of *COX-1* ($p = 0.06$) (Fig. 2C, E, F, and G). However, in STZ-treated KO mice, *COX-2* and *mPGES-1* were elevated 200-fold and 7-fold, respectively, but the other enzymes (*COX-1*, *cPGES*, and *15-PGDH*) were unaffected. The regulation of *COX-2* mRNA expression was further confirmed by Western blotting (Fig. 2D). Interestingly, although mPGES-2 played a crucial role in the protection against STZ-induced liver injury, neither protein nor mRNA of mPGES-2 was affected by STZ (Fig. 2B and C).

Enhancement of liver apoptosis in mPGES-2 KO mice following STZ treatment

To evaluate the involvement of apoptosis in the aggravated liver injury in KO mice, we examined the expression of caspase-3, BAX, and BAK using qRT-PCR and Western blotting. STZ induced a significant increase of *BAX* mRNA (WT/cont 1.02 ± 0.13 *vs.* WT/STZ4.71 ± 0.70, $p < 0.01$) and slight increases of caspase-3 (WT/control 1.06 ± 0.18 *vs.* WT/STZ 2.62 ± 1.0, $p > 0.05$) and *BAK* mRNAs (WT/control 1.20 ± 0.45 *vs.* WT/STZ 1.83 ± 0.49, $p > 0.05$) in WT mice with a much greater elevations of the apoptotic gene expression in STZ-treated KO mice (Fig. 2J–L). The protein expressions of pro-caspase-3 and cleavage-caspase-3 in the liver were significantly upregulated by STZ in KO mice, but not in WT mice (Fig. 2I). The Bcl-2 protein was reduced in both WT and KO mice following STZ treatment with a tendency of greater reductions in KO mice (Fig. 2I). Since DNA fragmentation is a hallmark of apoptosis, we performed the DNA ladder analysis of liver tissue. As expected, STZ induced severe DNA fragmentation in liver tissues of KO mice, but not of WT mice (Fig. 2H).

Enhanced inflammation and oxidative stress in the liver of mPGES-2 KO mice after STZ treatment

Inflammation and oxidative stress were evaluated by examining the expression levels of pro-inflammatory cytokines, NADPH oxidase subunits/HO-1 expression levels, liver TBARS content, and

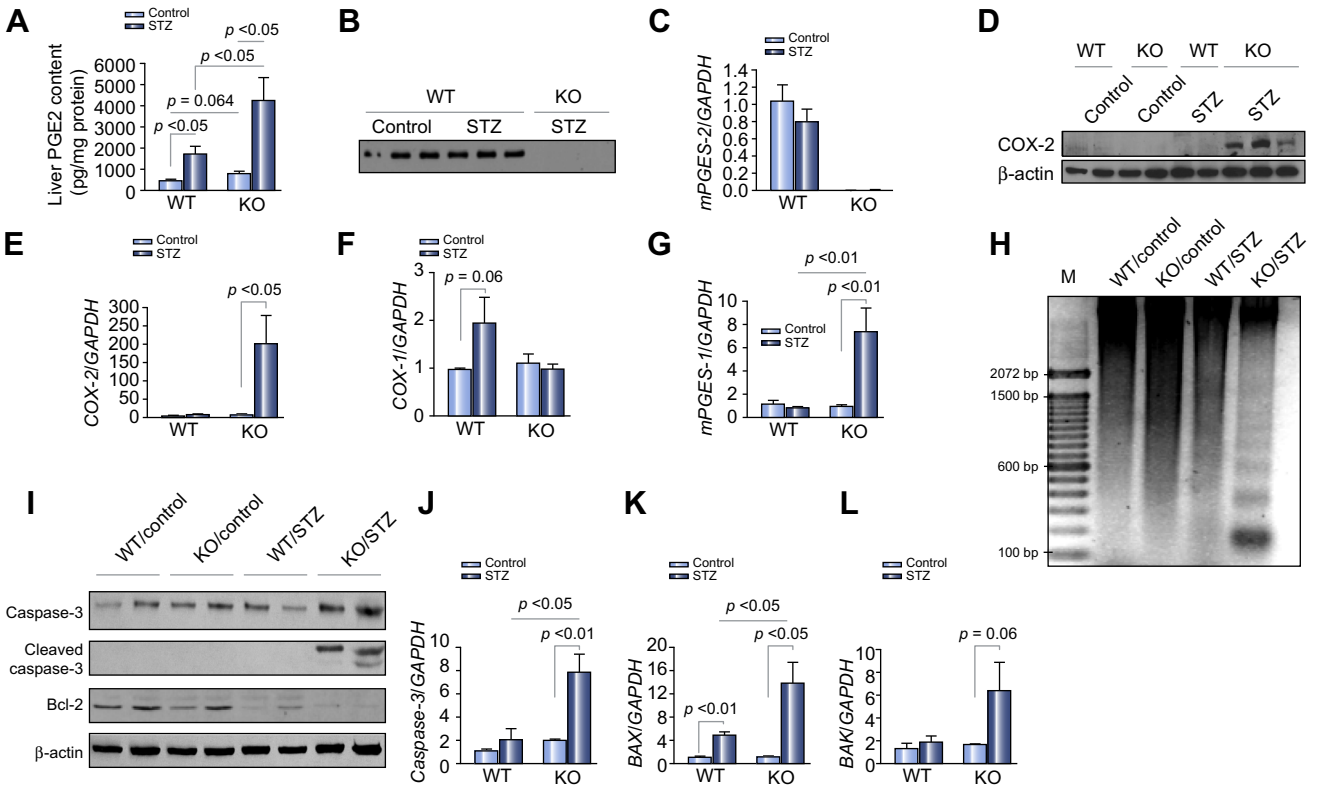

Fig. 2. Effect of mPGES-2 deletion on liver PGE_2 production and liver apoptosis after STZ treatment. (A) Liver PGE_2 content was measured by an enzyme immunoassay (EIA) assay. (B) Western blot analysis of liver mPGES-2 expression. (C) qRT-PCR of mPGES-2 in liver. (D) Western blot of COX-2 protein in liver. (E) qRT-PCR of *COX-2* in liver. (F) qRT-PCR of *COX-1* in liver. (G) qRT-PCR of *mPGES-1* in liver. (H) Liver DNA ladder. (I) Caspase-3 (Cas-3), cleaved caspase-3 (c-Cas-3), and Bcl-2 protein expressions were determined by Western blotting. (J) qRT-PCR of Caspase-3. (K) qRT-PCR of *BAX* in liver. (L) qRT-PCR of *BAK* in liver. n = 5–6 per group. WT, wild type; Cont, control. Data are means ± SE.

liver immunoreactivity of nitrotyrosine, respectively. By qRT-PCR, *TNF*-α and *MCP-1* mRNA levels were significantly elevated in mPGES-2 KO mice after STZ treatment, whereas no obvious changes were observed in mPGES-2 WT mice (*TNF-α*: WT/control 1.28 ± 0.5 *vs.* WT/STZ 1.72 ± 0.33, $p > 0.05$ and KO/control 0.8 ± 0.12 *vs.* KO/STZ 7.6 ± 3.3, $p < 0.05$; *MCP-1*: WT/control 1.08 ± 0.22 *vs.* WT/STZ 7.5 ± 3.16, $p > 0.05$ and KO/control 1.26 ± 0.22 *vs.* KO/STZ 253.64 ± 89.8, $p < 0.05$) (Fig. 3A and B). By Western blotting, TNF-α protein was significantly increased by STZ in the liver of WT mice contrasting the unaltered mRNA level (Fig. 3C and D). In parallel with the liver morphological and functional changes, the KO mice showed a greater induction of liver TNF-α following the STZ treatment in comparison with the WT (Fig. 3C and D). By ELISA assay, we found a significant induction of IL-1β in KO mice but not in WT mice (Fig. 3E).

The NADPH oxidase subunits *p47phox* (WT/control 1.02 ± 0.11 *vs.* WT/STZ 1.16 ± 0.23, $p > 0.05$; KO/control 0.92 ± 0.06 *vs.* KO/STZ 4.5 ± 1.36, $p < 0.05$) and *p67phox* (WT/control 1.06 ± 0.21 *vs.* WT/STZ 1.86 ± 0.39, $p > 0.05$; KO/control 1.02 ± 0.06 *vs.* KO/STZ 5.9 ± 1.69, $p < 0.05$) mRNA levels were significantly enhanced in KO mice but not in WT controls (Fig. 3F and G). HO-1, an oxidative stress marker, was also significantly increased in mPGES-2 KO mice but not WT mice, as determined by qRT-PCR and Western blotting (Fig. 3H–J). We further examined liver TBARS and the immunoreactivity of nitrotyrosine and found both of them were robustly increased in the liver of KO mice but not WT mice after 3 days of STZ injection (Fig. 3K and L).

Evaluation of pancreas injury

Three days after STZ i.p. injection, the increase in blood glucose was similar between the two genotypes, suggesting a similar degree of injury to pancreatic β-cells. Meanwhile, WT and KO mice showed comparable plasma insulin levels (WT/STZ: 0.452 ± 0.15 ng/ml *vs.* KO/STZ: 0.454 ± 0.05 ng/ml, $p > 0.05$) after 3 days STZ injection. Consistent with these observations, the indices of inflammation and apoptosis including pancreatic expression of TNF-α, MCP-1, caspase-3, or BAX in response to STZ treatment were unaffected by mPGES-2 deficiency (Supplementary Fig. 2E–H).

Effect of mPGES-2 deletion on the regulation of GLUT2, SREBP-1c and the insulin signalling pathway

To further study the potential involvement of liver glucose transporters in the regulation of the glucose metabolism, we examined the expression of GLUT2, the principle glucose transporter in the liver and found a liver-specific elevation of both GLUT2 protein and mRNA levels in KO mice under normal conditions (Fig. 4B and Supplementary Fig. 3F). In contrast, no increments were detected in pancreas and kidney of KO mice (Supplementary Fig. 3A and B). By immunohistochemistry, GLUT2 was localized at the sinusoidal plasma membrane of hepatocytes in WT mice and a stronger expression of GLUT2 immunoreactivity was detected in mPGES-2 KO mice (Fig. 4A and Supplementary

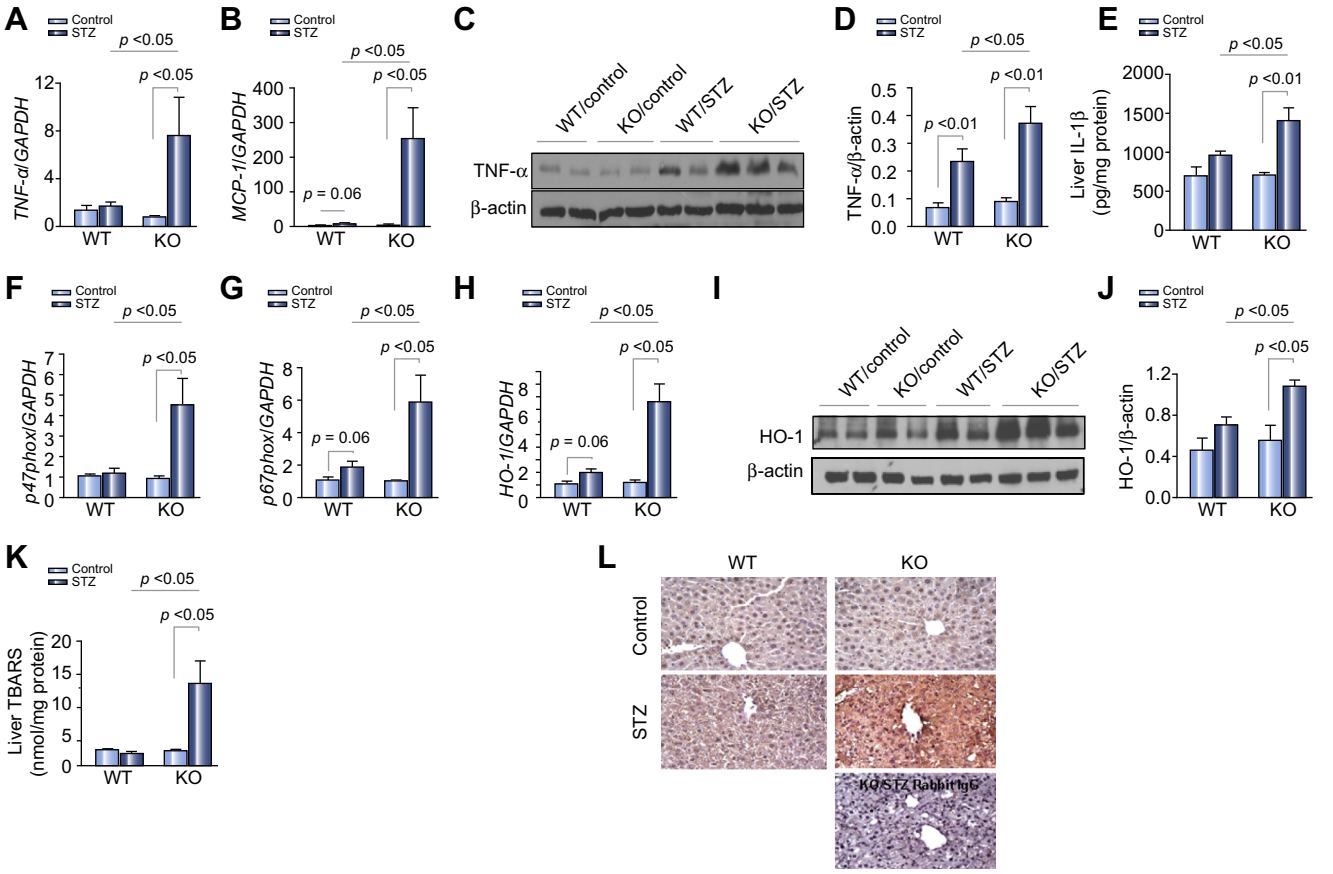

Fig. 3. mPGES-2 deletion enhanced inflammation and oxidative stress in the liver. (A) qRT-PCR of *TNF1-α*. (B) qRT-PCR of *MCP-1*. (C) Western blot of TNF-α proteins. (D) Quantification of liver TNF-α proteins. (E) Liver IL-1β content. (F–H) mRNA levels of liver *p47phox* (F), *p67phox* (G), and *HO-1* (H) were determined by real-time qPCR. (I) Western blot of HO-1. (J) Quantification of liver HO-1 protein expression. (K) Liver TBARS content. (L) Immunohistochemistry of nitrotyrosine. n = 5–6 per group. Data are means ± SE. (This figure appears in colour on the web.)

Fig. 3F). We further analysed GLUT1 and GLUT4 expressions by qRT-PCR in the liver and found no difference between WT and KO mice (Supplementary Fig. 3D and E). After 3 days of STZ treatment, GLUT2 and GLUT4, but not GLUT1, were markedly reduced to identical levels (Supplementary Fig. 3C and E). Next, we examined the SREBP-1c, a known activator of GLUT2, by Western blotting. As shown by Supplementary Fig. 7B and C, mPGES-2 deletion markedly increased the expression of SREBP-1c in control mice. Finally, we measured expressions of the insulin receptor-β (IR-β) and the phosphorylation of AKT (p-AKT). Importantly, both IR-β and p-AKT were upregulated in the liver of KO mice under basal conditions (Supplementary Fig. 7A). These results highly suggested increased insulin sensitivity in KO mice at least in liver tissue. To further validate this hypothesis, we performed a glucose tolerance test (GTT) and insulin tolerance test (ITT) in these animals. As expected, both GTT and ITT were significantly improved in KO mice (Supplementary Fig. 7D and E).

Evaluation of lipid metabolic enzymes in the liver

Considering the lipid accumulation in the liver of mPGES-2 KO mice, we analysed lipid metabolism-related enzymes including *DGAT1*, *DGAT2*, *HTGL*, and *FAS* in liver tissue by qRT-PCR. Strikingly, all these enzymes were reduced after 3 days of STZ treatment in both genotypes with a greater reduction of *DGAT2* and *HTGL* in KO mice (Supplementary Fig. 4A–D). However, under the baseline condition, all these enzymes are comparable between genotypes except for *HTGL* showing a 2.7-fold mRNA enhancement in KO mice (Supplementary Fig. 4C). Finally, we analysed PPARα, a transcription factor and key regulator of lipid metabolism in liver, and found a robust reduction of *PPARα* mRNA expression in KO mice after 3 days STZ administration contrasting the unaltered expression in WT mice (Supplementary Fig. 4E). These results suggested that lipid accumulation in hepatocytes could be secondary to cell injury rather than a causative factor leading to the liver damage.

In vitro studies

To further investigate the cellular mechanisms involved in the hepatic phenotype of STZ-treated mPGES-2 KO mice, we performed a series of *in vitro* experiments using primary hepatocytes from mPGES-2 WT and KO mice. After 24-h STZ treatment at various concentrations, mPGES-2 KO hepatocytes exhibited increased sensitivity to STZ-induced cell damage as determined by the MTT assay (Fig. 4C). Similarly to the MTT results, the LDH cytotoxicity assay showed significantly increased cell injury (Fig. 4D). As shown in Fig. 4E, pro-caspase-3 was elevated by STZ

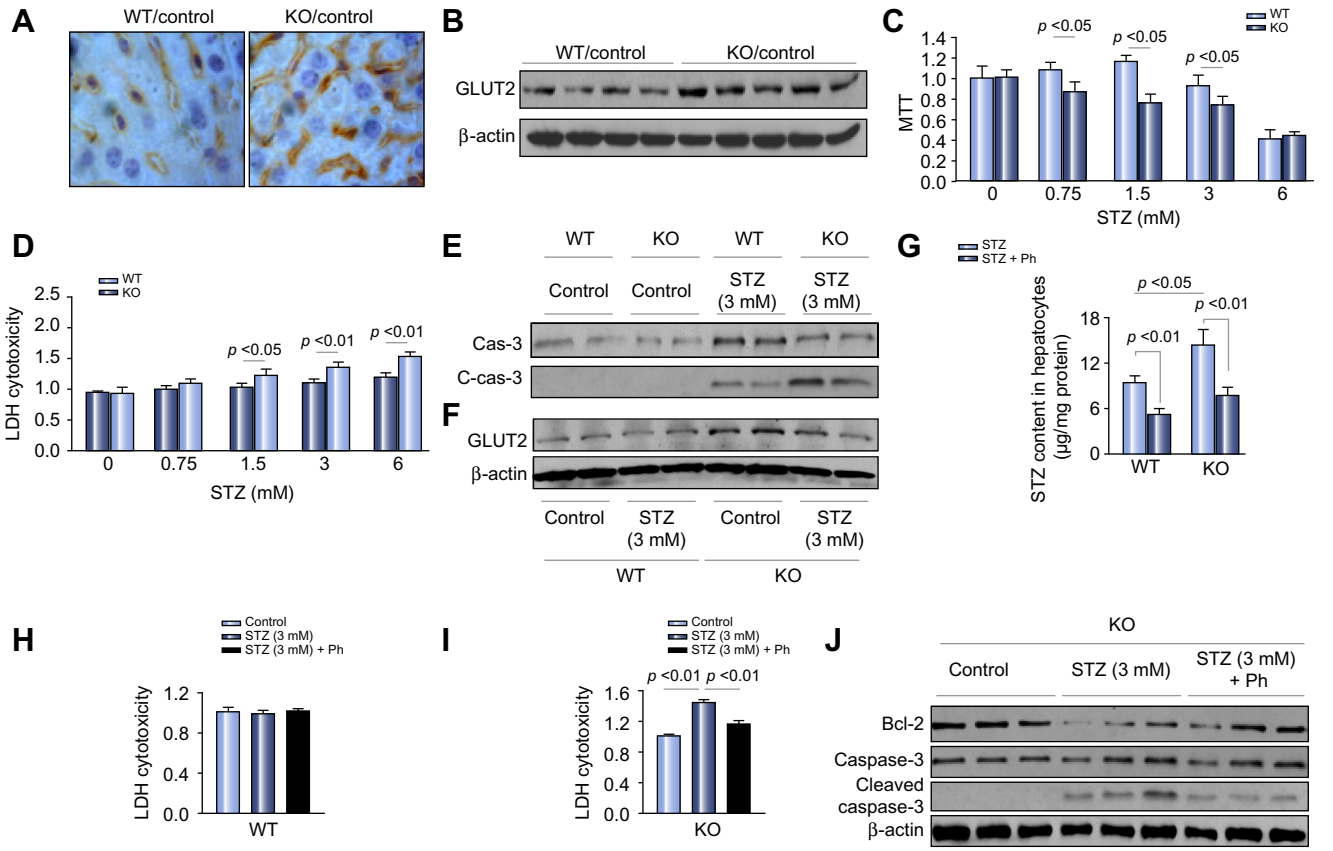

Fig. 4. Upregulation of GLUT2 mediated enhanced hepatotoxicity of STZ in mPGES-2 KO mice. (A) Immunohistochemistry of liver GLUT2 in mPGES-2 WT and KO control mice. (B) Western blotting analysis of liver GLUT2 in mPGES-2 WT and KO mice. n = 9–10 in each group. (C) MTT analysis for the cell viability with 0 mM, 0.75 mM, 1.5 mM, 3 mM and 6 mM STZ for 24 h (n = 6). (D) LDH cytotoxicity (n = 6 per group). (E and F) Western blot of caspase-3 (Cas-3), cleaved caspase-3 (c-Cas-3) (E), and GLUT2 (F) expressions in mPGES-2 WT and KO hepatocytes treated with or without STZ (3 mM); n = 3 per group. (G) STZ concentration was measured in mPGES-2 WT and KO hepatocytes after STZ (6 mM) treatment for 90 min with or without pretreatment of phloretin (20 μM); n = 5–7 per group. (H and I) LDH cytotoxicity was determined in mPGES-2 WT (H) and KO hepatocytes (I) treated by 3 mM STZ with or without 20 μM phloretin for 24 h; n = 3 per group. (J) Immunoblot of Bcl-2, Caspase-3, and cleaved caspase-3 expressions in mPGES-2 deficient hepatocytes treated by 3 mM STZ with or without 20 μM phloretin for 24 h; n = 3 per group. Data are means ± SE. (This figure appears in colour on the web.)

in WT but not in mPGES-2 KO hepatocytes, while the active caspase-3 (cleaved form) was much higher in the KO cells suggesting an increased apoptotic response to STZ in mPGES-2 deficient cells.

As has been seen in liver tissue *in vivo*, GLUT2 expression in primary mPGES-2 KO hepatocytes remained elevated compared with the WT cells (Fig. 4F). To test the contribution of elevated GLUT2 for the increased cytotoxicity of STZ in the KO cells, we treated the cells with the selective GLUT2 inhibitor phloretin. As shown in Fig. 4G, the STZ content was significantly higher in mPGES-2 KO cells than WT cells, and phloretin treatment markedly reduced STZ content in both WT and KO cells. The LDH cytotoxicity assay showed that the STZ-induced cellular LDH release was significantly reversed by GLUT2 inhibition (Fig. 4I and Supplementary Fig. 5C). In WT cells, both STZ and phloretin played no role in LDH release (Fig. 4H). Accordingly, the downregulation of Bcl-2 and upregulation of cleaved caspase-3 by 3 mM STZ were partially but significantly reversed by phloretin administration (Fig. 4J). Later, we evaluated the effect of phloretin on cellular TG accumulation following STZ treatment and observed a 2-fold increase of cellular TG content in KO but not in WT cells, and such an increment was entirely abolished by phloretin at a dose of 20 μM (Supplementary Fig. 5A and B). At last, we looked at the expressions of DGAT1, DGAT2, and HTGL in cells. DGAT2 was reduced by STZ in contrast to an induction of HTGL in KO but not in WT cells. However, DGAT1 was not affected by STZ in both WT and KO cells (Supplementary Fig. 6A–C). Altogether, these results suggest that the upregulation of GLUT2 in mPGES-2 KO hepatocytes is at least in part responsible for the enhanced hepatocyte injury induced by STZ. The accumulation of TG in KO cells is possibly secondary to the STZ-induced cellular injury.

Role of mPGES-2 in the CCl_4-induced liver injury model

We generated another liver injury model using CCl_4 to clarify if the liver protective effect of mPGES-2 is universal under different pathological conditions. Unlike the STZ model, CCl_4 caused similar histological lesions between WT and KO mice (Supplementary Fig. 8A and B), paralleled with comparable elevations of AST and ALT (Supplementary Fig. 8C).

Discussion

mPGES-2 has been cloned for more than 10 years as a PGE synthase. Early studies related to its action in PGE_2 synthesis were

all performed *in vitro* and claimed that its PGE_2 synthetic activity is independent of GSH [2]. However, recent study in mPGES-2 KO mice failed to validate its PGE2 synthase activity [6]. Most recently, a study by Takusagawa convincingly and innovatively demonstrated that mPGES-2 is a GSH-dependent, haem-bound protein and only haem-free mPGES-2 presents the capability of PGE_2 synthesis under *in vitro* conditions [5]. It is imaginable that the *in vivo* environment is haem-enriched and the haem-free form of mPGES-2 probably does not exist *in vivo*. This may be a reasonable explanation why the PGE_2 content was not altered by mPGES-2 deletion. And it suggested a possibility that mPGES-2 may play important roles independently of PGE_2. In agreement with this hypothesis, the liver PGE_2 content in KO mice showed a higher tendency at baseline and a much greater PGE_2 induction in parallel with the robust elevations of COX-2 and mPGES-1 following 3 days of STZ treatment. This remarkable activation of the COX-2/mPGES-2/PGE_2 pathway in STZ-treated KO mice is possibly secondary to the STZ-induced liver damage.

The *PTGES2* (mPGES-2) gene location is close to chromosome band 9q34.13 which is closely linked to obesity [7]. Emerging evidence demonstrated a close association between *PTGES2* Arg298His polymorphism and type-2 diabetes [8–11]. To evaluate the role of mPGES-2 in diabetes, we treated mPGES-2 WT and KO mice with a single injection of STZ. Unexpectedly, mPGES-2 KO mice exhibited increased sensitivity to STZ-induced liver toxicity associated with high lethality. The STZ-treated KO mice had globally a yellowish liver and enlarged stomach contrasting the WT controls, which had no any noticeable abnormalities in liver and stomach. The data from PAS staining, EM, Oil Red O staining, and biochemical assay of the liver TG content indicated a global hepatic steatosis in KO mice accompanied with highly elevated liver enzymes of AST and ALT. However, the mRNA regulation of lipid metabolic enzymes and *PPARα* from both *in vivo* and *in vitro* studies highly suggested that the fatty liver of STZ-treated KO mice is possibly secondary to the cell injury rather than a primary insult, leading to lethal liver failure. At the same time, the stomach wall in KO mice turned out to be extremely thin as shown by PAS staining. In consideration of the extremely severe damage of the whole liver, acute hepatic failure may serve as a major cause of the lethality. The stomach enlargement is possibly secondary to severe hepatic failure but a direct effect on the stomach cannot be ruled out.

The mechanism of STZ cytotoxicity is well documented in pancreatic β-cells but is poorly understood in other organs including the liver and kidney. In pancreatic β-cells, GLUT2 is most abundant and is responsible for the transport of STZ into cells [21–24]. STZ is highly genotoxic via direct methylation of DNA, producing extensive DNA strand breaks and cell apoptosis in pancreatic β-cells [17,25]. Moreover, STZ was also shown to cause DNA fragmentation in the liver and kidney [26,27]. However, the injury in liver and kidney is relatively minor compared with pancreatic islets possibly due to the lower abundance of GLUT2 in these organs. To investigate if the STZ-induced DNA damage was worse in the liver of mPGES-2 KO mice, we performed a DNA ladder assay and examined the expression of apoptotic genes. As expected, the mPGES-2 KO mice showed a greater induction of *caspase-3*, *BAK*, and *BAX* mRNA levels and a robust induction of cleaved-caspase-3. Along this line, the severe DNA fragmentation was detected only in KO but not WT mice after STZ treatment. Moreover, the inflammation and oxidative stress levels in KO mice, as reflected by the inflammatory markers TNF-α, MCP-1, and IL-1β and the oxidative stress markers of p47phox, p67phox, HO-1, TBARS, and nitrotyrosine, respectively, were also much greater in KO mice than in the WT control.

In the present study, GLUT2, but not GLUT1 and GLUT4, was selectively upregulated in the liver upon mPGES-2 deficiency under normal conditions. After 3 days of STZ treatment, GLUT2 and GLUT4 were robustly downregulated to similar levels in both genotypes. This interesting finding suggests that GLUT2 upregulation may serve as the leading cause of abnormal STZ accumulation and finally lead to the observed lethal liver damage. To elucidate whether GLUT2 plays a crucial role in mediating abnormal STZ accumulation and lethal liver damage, we performed *in vitro* studies using primary cultured hepatocytes from mPGES-2 WT and KO mice. As expected, mPGES-2 KO cells exhibited higher sensitivity to STZ-induced injury than WT controls. The cellular STZ content in KO cells was significantly higher than in WT cells and this increase was remarkably attenuated by pretreatment with a selective GLUT2 inhibitor. In response to the GLUT2 inhibition, STZ-induced cell injury, as assessed by the LDH cytotoxicity assay, cellular lipid accumulation, and evaluation of apoptosis markers were almost completely reversed by GLUT2 inhibition in the KO cells. This *in vitro* evidence suggests that the enhancement of a GLUT2-dependent transport of STZ in hepatocytes may largely contribute to the increased sensitivity of mPGES-2 KO mice to STZ-induced liver toxicity. Although phloretin is capable to inhibit the activity of other glucose transporters besides GLUT2 [28,29], the hundreds to thousands times higher levels of GLUT2 compared to other glucose transporters in the liver [30] could lead to a higher sensitivity of GLUT2 to phloretin in hepatocytes, particularly in the mPGES-2 KO cells with greater GLUT2 expression. Moreover, it is known that GLUT2 is the principle glucose transporter responsible for transporting STZ into the cells. Thus, the attenuation of STZ accumulation by phloretin could be due to the blockade of GLUT2 activity, which subsequently ameliorated hepatocyte injury.

Pancreatic β-cells are the major target of STZ. Following 3 days of STZ treatment, mPGES-2 WT and KO mice developed a similar degree of hyperglycemia in parallel with comparable plasma insulin levels. Consistent with these results, there was no significant difference in the indices of inflammation and apoptosis in the pancreatic tissue between mPGES-2 WT and KO mice, nor was the expression of GLUT2 different in this tissue. However, the baseline level of plasma insulin was significantly higher in KO mice compared with WT controls, which indicated a suppressive role of mPGES-2 in mediating the insulin production and/or secretion in islet β-cells. These data suggested that diabetes per se as a result of the pancreatic β-cells injury may not be a contributing factor of the increased sensitivity of STZ-induced liver toxicity in mPGES-2 KO mice.

It is known that GLUT2 is positively regulated by SREBP-1c, enhancing the GLUT2 promoter activity in hepatocytes [31]. Moreover, insulin has been shown to be a potent stimulator of SREBP-1c in hepatocytes [32–34]. Interestingly, a most recent publication by Selda *et al.* reported that insulin increased GLUT2 via AKT in the liver [35]. In our mPGES-2 KO mice, we found a 2-fold elevation of the plasma insulin concentration under baseline conditions in parallel with a significant stimulation of insulin signalling and SREBP-1c expression in the liver. Based on the known evidence and our findings, we conclude that the upregulation of liver GLUT2 in mPGES-2 KO mice is possibly through the insulin/SREBP-1c pathway.

To test whether mPGES-2 exerts a broad protective role in different types of liver injury, we generated another liver injury model in mPGES-2 KO mice by using CCl_4. It is well known that CCl_4 induces liver injury through generation of reactive oxygen species (ROS) [36,37]. Our results revealed no obvious difference in the increases in plasma AST and ALT levels between WT and KO mice after exposure to CCl_4, suggesting a similar hepatocellular injury, irrespective of the genotype. Consistent with the serum enzyme results, the histological analysis further showed similar lesions in mPGES-2 WT and KO mice. Together, these results support the specific role of mPGES-2 in liver toxicity associated with STZ but not with CCl_4.

In summary, our findings demonstrate that mPGES-2 deficiency robustly increased STZ-induced liver toxicity possibly via the increase of GLUT2-dependent uptake of STZ. STZ is a FDA-approved drug for treating cancer of the pancreatic islet cells but toxicity has limited its application. Our results suggest that mPGES-2 activation may serve as a novel intervention to limit STZ toxicity, particularly in liver, thereby expanding the therapeutic window of STZ.

Financial support

This work was supported by the National Institutes of Health Grant DK094956, National Natural Science Foundation of China Grant No. 31330037, VA Merit Review, and National Basic Research Program of China 973 Program 2012CB517600 (No. 2012CB517602), and a Scientist Development Grant from the American Heart Association (11SDG7480006). T. Yang is an Established Investigator from the American Heart Association and Research Career Scientist in the Department of Veterans Affairs.

Conflict of interest

The authors who have taken part in this study declared that they do not have anything to disclose regarding funding or conflict of interest with respect to this manuscript.

Supplementary data

Supplementary data associated with this article can be found, in the online version, at http://dx.doi.org/10.1016/j.jhep.2014.07.018.

References

[1] Watanabe K, Kurihara K, Suzuki T. Purification and characterization of membrane-bound prostaglandin E synthase from bovine heart. Biochim Biophys Acta 1999;1439:406–414.
[2] Tanikawa N, Ohmiya Y, Ohkubo H, Hashimoto K, Kangawa K, Kojima M, et al. Identification and characterization of a novel type of membrane-associated prostaglandin E synthase. Biochem Biophys Res Commun 2002;291:884–889.
[3] Murakami M, Nakashima K, Kamei D, Masuda S, Ishikawa Y, Ishii T, et al. Cellular prostaglandin E2 production by membrane-bound prostaglandin E synthase-2 via both cyclooxygenases-1 and -2. J Biol Chem 2003;278:37937–37947.
[4] Yang G, Chen L, Zhang Y, Zhang X, Wu J, Li S, et al. Expression of mouse membrane-associated prostaglandin E2 synthase-2 (mPGES-2) along the urogenital tract. Biochim Biophys Acta 2006;1761:1459–1468.
[5] Takusagawa F. Microsomal prostaglandin E synthase type 2 (mPGES2) is a glutathione-dependent heme protein, and dithiothreitol dissociates the bound heme to produce active prostaglandin E2 synthase in vitro. J Biol Chem 2013;288:10166–10175.
[6] Jania LA, Chandrasekharan S, Backlund MG, Foley NA, Snouwaert J, Wang IM, et al. Microsomal prostaglandin E synthase-2 is not essential for in vivo prostaglandin E2 biosynthesis. Prostaglandins Other Lipid Mediat 2009;88:73–81.
[7] Wilson AF, Elston RC, Tran LD, Siervogel RM. Use of the robust sib-pair method to screen for single-locus, multiple-locus, and pleiotropic effects: application to traits related to hypertension. Am J Hum Genet 1991;48:862–872.
[8] Fisher E, Nitz I, Lindner I, Rubin D, Boeing H, Mohlig M, et al. Candidate gene association study of type 2 diabetes in a nested case-control study of the EPIC-Potsdam cohort – role of fat assimilation. Mol Nutr Food Res 2007;51:185–191.
[9] Lindner I, Helwig U, Rubin D, Fischer A, Marten B, Schreiber S, et al. Prostaglandin E synthase 2 (PTGES2) Arg298His polymorphism and parameters of the metabolic syndrome. Mol Nutr Food Res 2007;51:1447–1451.
[10] Nitz I, Fisher E, Grallert H, Li Y, Gieger C, Rubin D, et al. Association of prostaglandin E synthase 2 (PTGES2) Arg298His polymorphism with type 2 diabetes in two German study populations. J Clin Endocrinol Metab 2007;92:3183–3188.
[11] Fischer A, Grallert H, Bohme M, Gieger C, Boomgaarden I, Heid I, et al. Association analysis between the prostaglandin E synthase 2 R298H polymorphism and body mass index in 8079 participants of the KORA study cohort. Genet Test Mol Biomarkers 2009;13:223–226.
[12] Eizirik DL, Pipeleers DG, Ling Z, Welsh N, Hellerstrom C, Andersson A. Major species differences between humans and rodents in the susceptibility to pancreatic beta-cell injury. Proc Natl Acad Sci USA 1994;91:9253–9256.
[13] Schnedl WJ, Ferber S, Johnson JH, Newgard CB. STZ transport and cytotoxicity. Specific enhancement in GLUT2-expressing cells. Diabetes 1994;43:1326–1333.
[14] Elsner M, Guldbakke B, Tiedge M, Munday R, Lenzen S. Relative importance of transport and alkylation for pancreatic beta-cell toxicity of streptozotocin. Diabetologia 2000;43:1528–1533.
[15] Yang H, Wright Jr JR. Human beta cells are exceedingly resistant to streptozotocin in vivo. Endocrinology 2002;143:2491–2495.
[16] Dufrane D, van Steenberghe M, Guiot Y, Goebbels RM, Saliez A, Gianello P. Streptozotocin-induced diabetes in large animals (pigs/primates): role of GLUT2 transporter and beta-cell plasticity. Transplantation 2006;81:36–45.
[17] Yamamoto H, Uchigata Y, Okamoto H. Streptozotocin and alloxan induce DNA strand breaks and poly(ADP-ribose) synthetase in pancreatic islets. Nature 1981;294:284–286.
[18] Burkart V, Wang ZQ, Radons J, Heller B, Herceg Z, Stingl L, et al. Mice lacking the poly(ADP-ribose) polymerase gene are resistant to pancreatic beta-cell destruction and diabetes development induced by streptozocin. Nat Med 1999;5:314–319.
[19] Masutani M, Suzuki H, Kamada N, Watanabe M, Ueda O, Nozaki T, et al. Poly(ADP-ribose) polymerase gene disruption conferred mice resistant to streptozotocin-induced diabetes. Proc Natl Acad Sci USA 1999;96:2301–2304.
[20] Schmezer P, Eckert C, Liegibel UM. Tissue-specific induction of mutations by streptozotocin in vivo. Mutat Res 1994;307:495–499.
[21] Thorens B, Sarkar HK, Kaback HR, Lodish HF. Cloning and functional expression in bacteria of a novel glucose transporter present in liver, intestine, kidney, and beta-pancreatic islet cells. Cell 1988;55:281–290.
[22] Fukumoto H, Kayano T, Buse JB, Edwards Y, Pilch PF, Bell GI, et al. Cloning and characterization of the major insulin-responsive glucose transporter expressed in human skeletal muscle and other insulin-responsive tissues. J Biol Chem 1989;264:7776–7779.
[23] Bell GI, Kayano T, Buse JB, Burant CF, Takeda J, Lin D, et al. Molecular biology of mammalian glucose transporters. Diabetes Care 1990;13:198–208.
[24] Thorens B, Cheng ZQ, Brown D, Lodish HF. Liver glucose transporter: a basolateral protein in hepatocytes and intestine and kidney cells. Am J Physiol 1990;259:C279–C285.
[25] Okamoto H. Regulation of proinsulin synthesis in pancreatic islets and a new aspect to insulin-dependent diabetes. Mol Cell Biochem 1981;37:43–61.
[26] Kraynak AR, Storer RD, Jensen RD, Kloss MW, Soper KA, Clair JH, et al. Extent and persistence of streptozotocin-induced DNA damage and cell proliferation in rat kidney as determined by in vivo alkaline elution and BrdUrd labeling assays. Toxicol Appl Pharmacol 1995;135:279–286.

[27] Imaeda A, Kaneko T, Aoki T, Kondo Y, Nagase H. DNA damage and the effect of antioxidants in streptozotocin-treated mice. Food Chem Toxicol 2002;40:979–987.
[28] Ida-Yonemochi H, Nakatomi M, Harada H, Takata H, Baba O, Ohshima H. Glucose uptake mediated by glucose transporter 1 is essential for early tooth morphogenesis and size determination of murine molars. Dev Biol 2012;363:52–61.
[29] Vlachodimitropoulou E, Sharp PA, Naftalin RJ. Quercetin-iron chelates are transported via glucose transporters. Free Radic Biol Med 2011;50:934–944.
[30] Karim S, Adams DH, Lalor PF. Hepatic expression and cellular distribution of the glucose transporter family. World J Gastroenterol 2012;18:6771–6781.
[31] Im SS, Kang SY, Kim SY, Kim HI, Kim JW, Kim KS, et al. Glucose-stimulated upregulation of GLUT2 gene is mediated by sterol response element-binding protein-1c in the hepatocytes. Diabetes 2005;54:1684–1691.
[32] Jung YA, Kim HK, Bae KH, Seo HY, Kim HS, Jang BK, et al. Cilostazol inhibits insulin-stimulated expression of sterol regulatory binding protein-1c via inhibition of LXR and Sp1. Exp Mol Med 2014;46:e73.
[33] Chen G, Liang G, Ou J, Goldstein JL, Brown MS. Central role for liver X receptor in insulin-mediated activation of Srebp-1c transcription and stimulation of fatty acid synthesis in liver. Proc Natl Acad Sci USA 2004;101:11245–11250.
[34] Cagen LM, Deng X, Wilcox HG, Park EA, Raghow R, Elam MB. Insulin activates the rat sterol-regulatory-element-binding protein 1c (SREBP-1c) promoter through the combinatorial actions of SREBP, LXR, Sp-1 and NF-Y cis-acting elements. Biochem J 2005;385:207–216.
[35] Gezginci-Oktayoglu S, Sacan O, Bolkent S, Ipci Y, Kabasakal L, Sener G, et al. Chard (*Beta vulgaris* L. var. cicla) extract ameliorates hyperglycemia by increasing GLUT2 through Akt2 and antioxidant defense in the liver of rats. Acta Histochem 2014;116:32–39.
[36] Recknagel RO, Glende Jr EA, Dolak JA, Waller RL. Mechanisms of carbon tetrachloride toxicity. Pharmacol Ther 1989;43:139–154.
[37] Williams AT, Burk RF. Carbon tetrachloride hepatotoxicity: an example of free radical-mediated injury. Semin Liver Dis 1990;10:279–284.